Wollastonite-containing glass-ceramics from the CaO–Al2O3–SiO2 and CaO–MgO–SiO2 ternary systems

Open Ceramics 17 (2024) 100507

Contents lists available at ScienceDirect

Open Ceramics

journal homepage: www.sciencedirect.com/journal/open-ceramics

Wollastonite-containing glass-ceramics from the $CaO–Al_2O_3–SiO_2$ and $CaO–MgO–SiO_2$ ternary systems

Dilshat U. Tulyaganov [a], Konstantinos Dimitriadis [b], Simeon Agathopoulos [c], Francesco Baino [d], Hugo R. Fernandes [e,*]

[a] Turin Polytechnic University in Tashkent, 17 Small Ring Street, Tashkent, 100095, Uzbekistan
[b] Division of Dental Technology, Department of Biomedical Sciences, University of West Attica, Athens, Greece
[c] Department of Materials Science and Engineering, University of Ioannina, 451 10, Ioannina, Greece
[d] Institute of Materials Physics and Engineering, Applied Science and Technology Department, Politecnico di Torino, Corso Duca degli Abruzzi 24, 10129, Torino, Italy
[e] Department of Materials and Ceramic Engineering, CICECO, University of Aveiro, 3810-193 Aveiro, Portugal

ARTICLE INFO

Handling Editor: Dr P Colombo

Keywords:
Wollastonite
Phase diagrams
$CaO–Al_2O_3–SiO_2$ and $CaO–MgO–SiO_2$ systems
Glasses
Glass-ceramics

ABSTRACT

Glass-ceramics (GCs) are polycrystalline materials produced from parent glasses by the controlled crystallization that results in crystalline phase(s) embedded in a residual amorphous matrix. Typically, GCs are produced by a conventional glass route with subsequent crystallization for which two heat treatments are usually applied, the former to generate nuclei and the latter being a crystal growth stage. Alternatively, another technically viable route for manufacturing GCs involves sintering of glass-powder compacts followed by crystallization (sinter-crystallization).

Wollastonite-containing GCs from the $CaO–Al_2O_3–SiO_2$ and $CaO–MgO–SiO_2$ systems find a wide variety of uses in different technological fields, including construction, architecture, medical and high-tech fields. For example, a special type of wollastonite-containing GC marketed under the name of Neoparies®, which is stronger and lighter than natural stone, features high resistance to weathering/chemical attack and is manufactured on a large scale for construction and architectural applications. In the biomedical field, the well-known Cerabone® products have been used in bone-contact applications for many years.

The main goal of this brief review is to provide a critical analysis of the experimental trials focusing on the synthesis of wollastonite-containing GC materials and to discuss the various fields of their application. Constitution of phase diagram of $CaO–Al_2O_3–SiO_2$ and $CaO–MgO–SiO_2$ systems are comprehensively discussed with connection to melt crystallization path and crystalline phase formation. Furthermore, special emphasis will be given to the production of wollastonite-containing GCs for construction and architectural purposes from natural raw materials and wastes, as well as to the recent advancement in developing wollastonite-containing GC biomaterials for bone repair.

1. Introduction

The class of silicates encompasses the most abundant type of minerals on Earth. In fact, about 30 % of all minerals carry silicates and 90 % of the Earth's crust is composed of silicates [1]. The basic unit of silicates is the $(SiO_4)^{4-}$ tetrahedral anionic group; these tetrahedra can be linked to each other in different ways, thus forming single units, double units, chains, sheets, rings and framework structures. The richness in crystal structures makes silicates highly appealing and versatile materials that can be applied in multiple forms, including zeolites [2], mesoporous materials [3], inorganic-organic composites [4], etc. Silicates are also very important as raw precursors in glassmaking procedures and silicate crystalline phases can be found or deliberately developed in glass-ceramic materials deriving from a parent silica-based glass [5].

The subgroup of calcium silicates has gained remarkable attention due to the chemical and thermal stability of its belonging minerals, which find various applications in both traditional and high-tech fields including construction (*e.g.*, concrete production) and biomedicine (*e.g.*, bone repair and controlled drug delivery) [6–8]. Wollastonite ($CaSiO_3$), which is characterized by a fibrous structure of needle-like crystals, is

* Corresponding author.
E-mail address: h.r.fernandes@ua.pt (H.R. Fernandes).

https://doi.org/10.1016/j.oceram.2023.100507
Received 4 September 2023; Accepted 17 November 2023
Available online 20 November 2023

one of the most commonly used and representative members having low thermal conductivity and high dimensional stability, and being machinable, biocompatible and relatively inexpensive [9]. Noticeably, wollastonite-based GCs specifically discussed in the literature because those have achieved appropriate dielectric and optical properties and its potential influence on thermal barrier coatings [10–16].

This review specifically focuses on melt-derived partially-crystallized silicate glasses embedding wollastonite crystals that have been developed upon controlled thermal treatments. The production, properties and main applications of these materials synthesized in the $CaO–Al_2O_3–SiO_2$ and $CaO–MgO–SiO_2$ systems are presented and discussed, with focus on the construction and biomedical fields.

2. The phase diagram of the $CaO–Al_2O_3–SiO_2$ system

The phase diagram of the $CaO–Al_2O_3–SiO_2$ system according to Osborn and Maun [17] comprises two ternary compounds with congruent melting (*i.e.*, anorthite and gehlenite) and 10 binary compounds (Fig. 1). The first ternary compound is anorthite ($CaAl_2Si_2O_8$) that melts congruently at 1553 °C. It exists in three polymorphs: at high temperatures hexagonal and rhombic anorthites transform to ordinary triclinic one. In nature anorthite is presented as a common rock forming mineral of triclinic syngony with density of 2740–2760 kg.m^{-3}. Synthetic anorthite is produced through reaction in solid state or by crystallization of melt. Anorthite belongs to framework silicates formed from $[SiO_4]$ and $[AlO_4]$ tetrahedra between which Ca cations with coordination numbers 6 and 7 are located [17–19].

The second ternary compound is gehlenite ($Ca_2Al_2SiO_7$) that crystallized in tetragonal syngony and has melting point of 1593 °C. Gehlenite belongs to melilite family and forms continuous solid solutions along with akermanite ($Ca_2MgSi_2O_7$). Both gehlenite and akermanite are sorosilicates. The basic units of their structure formed through sharing of corner oxygens from tetrahedrons resulting in diorthogroups $Si_2O_7^{6-}$ that feature dimensions (4.1−4.2 Å) comparable with the edges of octahedral groups formed by larger cations like Ca^{2+}, Sr^{2+}, Ba^{2+}, etc. Some invariant points in the $CaO–Al_2O_3–SiO_2$ system are shown in Table 1.

Wollastonite is one of the binary compounds in the $CaO–Al_2O_3–SiO_2$ system with composition 48.3 wt% CaO and 51.7 wt% SiO_2 [20–23]. It was named by J. Léman in 1818 in honour of William Hyde Wollaston

Table 1
Some invariant points in the $CaO–Al_2O_3–SiO_2$ system.

	Equilibrium phases	Process	Composition (wt.%)			Temperature (°C)
			CaO	Al_2O_3	SiO_2	
1	$CaAl_2Si_2O_8$ (anorthite) + $CaSiO_3$ (wollastonite) + SiO_2 + liquid	Eutectic	23.2	14.8	62.0	1165
2	$CaAl_2Si_2O_8$ + $Al_6Si_2O_{13}$ (mullite) + SiO_2 + liquid	Eutectic	9.8	18.6	71.6	1345
3	$CaAl_2Si_2O_8$ + SiO_2 + liquid	Eutectic	10.2	18.5	71.3	1368
4	$CaAl_2Si_2O_8$ + $CaSiO_3$ + liquid	Eutectic	34.8	17.6	47.6	1307
5	$CaAl_2Si_2O_8$ + $CaSiO_3$ + $Ca_2Al_2SiO_7$ (gehlenite) + liquid	Eutectic	38	20	42	1265
6	$CaAl_2Si_2O_8$ + $Ca_2Al_2SiO_7$ (akermanite) + liquid	Eutectic	30.2	36.8	33	1387
7	$CaSiO_3$ + $Ca_2Al_2SiO_7$ + liquid	Eutectic	46.3	12.8	40.9	1318
8	$CaAl_2Si_2O_8$ + liquid	Melting	20.2	36.6	43.2	1553
9	$Ca_2Al_2SiO_7$ + liquid	Melting	42.5	36.2	21.3	1593
10	$CaSiO_3$ + liquid	Melting	48.3	–	51.7	1544

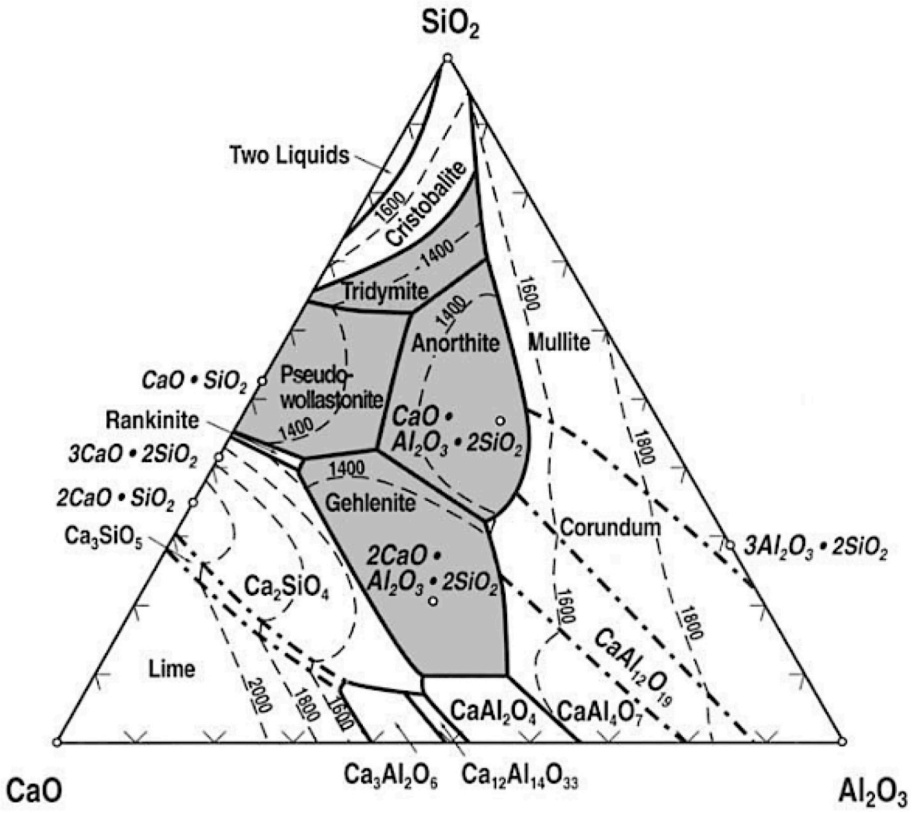

Fig. 1. Phase diagram of the $CaO–Al_2O_3–SiO_2$ system as reported by Osborn and Maun [17].

(1766–1828), famous English chemist and mineralogist [18]. Wollastonite belongs to the pyroxenoid group of minerals: pyroxenoids are often described as similar to the pyroxene group owing to the fact that both groups have a structure based on chains of SiO_4^{4-} tetrahedra (Fig. 2). In pyroxenes these chains are infinitely long and run parallel to the *z*-direction. This defines the length of the unit cell in the *z*-axis direction (*i.e.*, the *c* lattice parameter). Conversely, in pyroxenoids the chains have longer repeat patterns as 3, 5 and even longer [18,19]. Specifically [24], in wollastonite the repeat distance is three SiO_4^{4-} units, rather than a two-tetrahedra repeat in pyroxenes [24].

According to the United States Geological Survey (USGS), world reserves of wollastonite exceed 100 million tons: large deposits of wollastonite have been identified in China, Finland, India, Mexico, and the United States. Smaller, but significant, deposits have been identified in Canada, Chile, Kenya, Namibia, South Africa, Spain, Sudan, Tajikistan, Turkey, and Uzbekistan [25]. Other localities for the mining of wollastonite include Romania, Italy, Ireland, Norway, Germany, Canada, Japan [18]. Wollastonite exists in two polymorphic states: the low temperature triclinic form (β-$CaSiO_3$) converts to the high temperature form pseudo-wollastonite (α-$CaSiO_3$) at 1125 °C [23,26–29]. The coefficients of thermal expansion (CTEs) of α-$CaSiO_3$ and β-$CaSiO_3$ are 11.8 × 10^{-6} K^{-1} and 6.5 × 10^{-6} K^{-1}, respectively [30]. Naturally occurring wollastonite is mostly found as β-$CaSiO_3$ in thermally metamorphosed siliceous carbonates, intruding igneous rock, and skarn deposits along their contact. It may appear as white, grey-white, light green, pinkish, brown, red, yellow, transparent to translucent, vitreous or pearly, features perfect cleavage, uneven fracture, specific gravity 2860–3090 kg.m^{-3}, Mohs hardness 4.5–5, melts congruently at 1544 °C [18]. Both naturally occurring and artificial wollastonite reduce drying and firing shrinkage, promote lower moisture and thermal expansion in the fired product and increases firing strength. Wollastonite competes with carbonates, feldspar, lime, and silica as a source of calcium and silica and is used depending on the formulation of the ceramic body and the firing method [25,31].

The most fusible eutectics in the $CaO–Al_2O_3–SiO_2$ system with melting points 1165, 1265 and 1307 °C are adjacent to the fields of anorthite, gehlenite and wollastonite crystallization (Table 1). In melts with compositions located in wollastonite crystallization field and belonging to wollastonite-anorthite-silica triangle, wollastonite is crystallized first and then crystallization path goes along the boundary curve between wollastonite and anorthite up the eutectic point with a melting point of 1165 °C. Crystallization of melt ends in the eutectic point with the release of wollastonite, anorthite and quartz. Another combination of phases as wollastonite, anorthite and gehlenite will be formed upon crystallization of melts located in wollastonite crystallization field while belonging to wollastonite-anorthite-gehlenite triangle.

3. The phase diagram of the $CaO–MgO–SiO_2$ system

There are four ternary compounds in the $CaO–MgO–SiO_2$ system: diopside ($CaMgSiO_6$) and akermanite ($Ca_2MgSi_2O_7$) melt congruently at 1391 and 1454 °C, respectively, while monticellite ($CaMgSiO_4$) and mervinite ($Ca_3MgSi_2O_8$) melt incongruently at 1485 °C and 1575 °C, respectively. It was found that the increase in melting point of diopside with pressure can be represented by the expression $T_m = 1391.5 + 0.01297\ P$, where T_m is the melting temperature in °C and *P* is the pressure in bars [33]. Wollastonite (β-$CaSiO_3$) takes into solid solution as much as 21 % diopside, but little diopside (less than 5 %) enters into solid solutions in α-$CaSiO_3$ (pseudowollastonite). The inversion temperatures of β-$CaO–SiO_2$ (wollastonite) to α-$CaSiO_3$ is raised by solid solution of diopside from 1125 °C to 1368 °C [33]. The eutectic in binary diopside-wollastonite system is at 1358 °C and 62 % diopside, and the solid phases are wollastonite solid solutions containing 22 % diopside and pure diopside.

The phase relationships in the ternary system $CaO–MgO–SiO_2$ were investigated by Ferguson and Merwin [34]. Fig. 3 represents the phase diagram of $CaO–MgO–SiO_2$ system as reported by Osborn and Maun [17]. More information about crystalline phases, phase relationships and glassy materials synthesized in this system, their properties and application may be found elsewhere [35].

4. Synthesis and applications of wollastonite-containing glass-ceramics

Production of wollastonite-containing GCs in the systems $CaO–Al_2O_3–SiO_2$ and $CaO–MgO–SiO_2$ for construction and architectural purposes attracts interest due to easier fabrication, abundance of reagents, improved performance, and wide range of application [36–42]. Nippon Electric Glass Co., Ltd. produces Neopariés® GC with a marble-like appearance that is an ideal alternative to stone for interior and exterior usages in construction applications [42–44]. The principal raw materials used for preparation of Neopariés® GC is quartz sand,

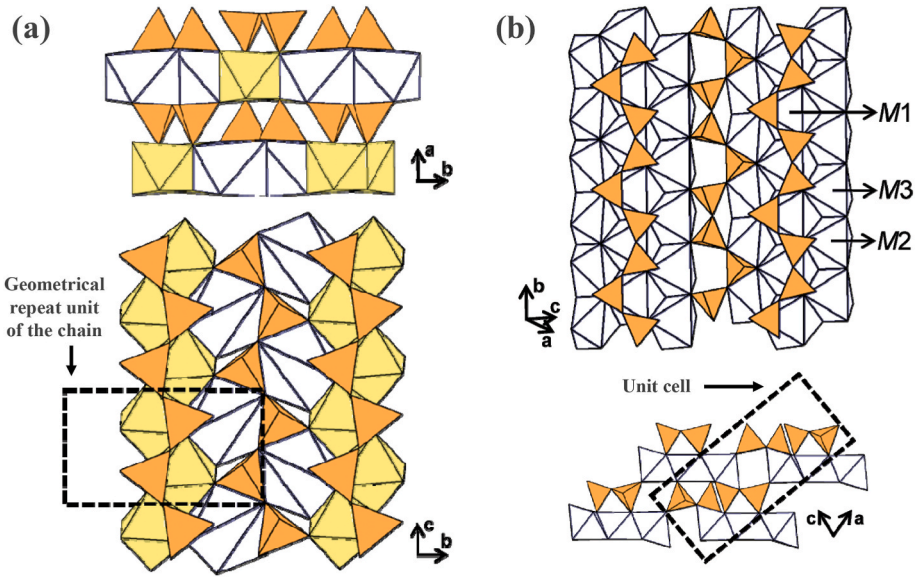

Fig. 2. The correlation of metasilicate (O/Si = 3) chains of [SiO_3] and bands of cations octahedrons: (a) for pyroxenes: diopside ($CaMg[Si_2O_6]$) and (b) for pyroxenoids: wollastonite ($Ca_3[Si_3O_9]$) (adapted from Ref. [32]).

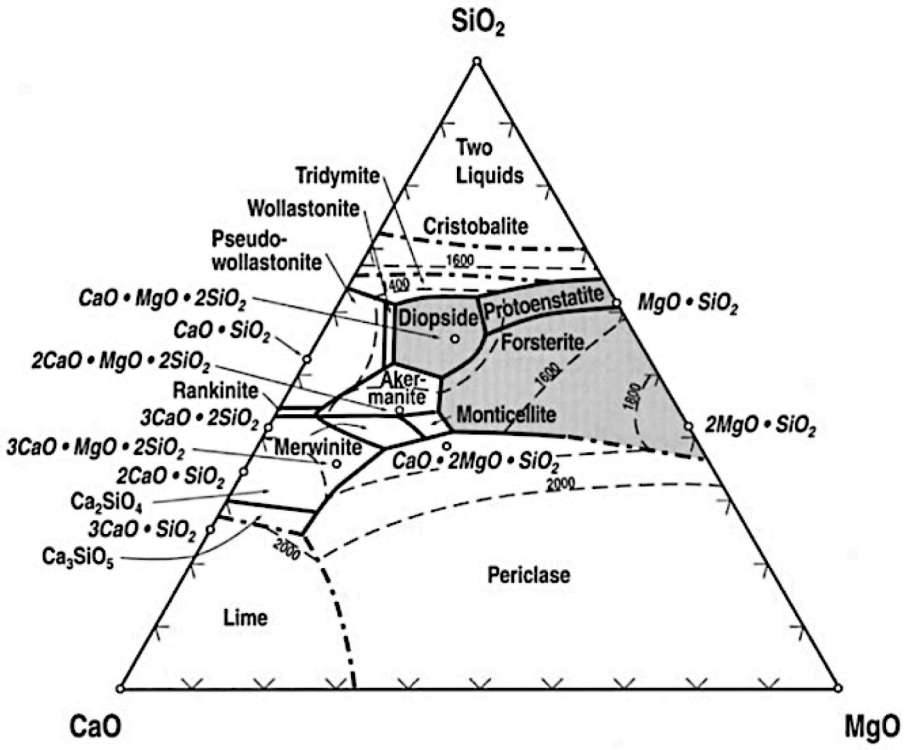

Fig. 3. Phase diagram of CaO–MgO–SiO_2 system as reported by Osborn and Maun [17].

sodium feldspar, calcium and barium carbonates. The chemical composition of the parent glass (in wt.%) is as follows: 59.1 SiO_2, 6.8 Al_2O_3, 19.1 CaO, 1.7 K_2O, 1.7 Na_2O, 0.6 B_2O_3, 6.8 ZnO and 4.3 BaO. This glass can be readily produced by melting the batch at 1400−1500 °C whilst viscosity of the melt is 10^2 P at 1440 °C, $10^{2.6}$ P at 1310 °C, 10^3 P at 1240 °C and 10^4 P at 1105 °C [42]. The parent glass demonstrates the following properties: density of 2780 kg.m^{-3}, a thermal expansion coefficient of 68.8 × 10^{-7} K^{-1}, a strain point of 628 °C and a softening point of 845 °C [42]. When small particles of this glass are heated at a rate of 2 K.min^{-1}, the softening of the glass begins at a temperature exceeding 850 °C causing the corner portion of the small particles to become round and deformed at further elevation of the temperature. At about 1000 °C surface crystallization is advanced and then, at about 1150 °C, crystals may grow from the surface toward the interior to about 1.5 mm. Upon 1 h holding at this temperature, β-wollastonite needle-like crystals may continue to grow to a length of about 5 mm, constituting 35 to 40 wt% of the bulk [42]. In industrial process the melt is quenched in water and the resulting glass frit with the sizes varying in the interval 1−7 mm is collected in a refractory mould plate of 100 × 100 cm^2 size. The accumulated glass products are slightly pressed so that the surface becomes flat. Heat treatment of the specimens is conducted in an electrical furnace at 2 K.min^{-1} to reach and then maintain the temperature of 1150 °C, followed by cooling at 1.7 K.min^{-1} to obtain a GCs with an aesthetic marble-like appearance. The final product features a smooth surface with a very beautiful pattern in which portions having a transparency and relatively white portions are tangled with each other (Fig. 4). Some properties of Neopariés® GC are shown in Table 2.

Fig. 4. The appearance of the Neopariés GC [43].

A GC with chemical composition very similar to Neopariés® (Table 3) was synthesized in Bulgaria [37,44]. The parent glass batch was prepared using 60 parts of dried incinerator fly ashes (MSWA), 25 parts of glass cullet, 25 parts of quartz sand and 4 parts of H_3BO_3 was prepared (as exactly as stated in Ref. [38]). The chemical composition of the glass (in wt.%) was as follows: 57.9 SiO_2, 6.9 Al_2O_3, 1.7 Fe_2O_3, 20.1 CaO, 3.5 MgO, 0.4 K_2O, 5.2 Na_2O, 0.1 PbO, 0.8 ZnO and 1.2 others. The sintering of glass granules was completed at low temperatures before the beginning of an intense phase formation process through surface crystallization. The temperature of maximum crystal growth rate was determined to be about 1020 °C [37,38].

Martin et al. investigated the feasibility of obtaining wollastonite-plagioclase GCs through crystallization of a parent glass made from glass fibers pyrolytically recovered from waste composites materials [40]. Glass frit was prepared at 1450 °C for 2 h. Samples were sinter-crystallized in the interval 850−1100 °C for 20 min. GCs sintered in the 1000−1030 °C range exhibited the highest bending strength values (122 MPa).

The possibility of effectively utilizing fly ash originated from a coal burning thermal power plant was investigated as a sustainable strategy to synthesize wollastonite-based GCs [45]. The base glass composition (G0) was 60.0 SiO_2, 8.0 Al_2O_3, 4.5 MgO, 18.5 CaO, 4.68 Fe_2O_3, 6.0 Na_2O, 1.06 K_2O (wt%). CaF_2 was added as a nucleating agent (G3 and G5) and spodumene [$LiAl(SiO_3)_2$] was also added (G5) for the reduction of the CTE by excess wt.%. Samples of each glass were prepared by

Table 2
Some properties of Neopariés® GC [42].

Properties	Neopariés GC	Natural marble	Natural granite
Density (kg.m^{-3})	2700	2700	2700
Bending strength (MPa)	42–44	3–25	15–17
Charpy impact strength	2.6–2.9	1.0–1.3	1.7–2.1
CTE (×10^{-7} K^{-1})	57	100–200	83

Table 3
Chemical composition of wollastonite-containing GCs (wt.%).

Glass	SiO_2	Al_2O_3/Fe_2O_3	CaO/ZnO	MgO/BaO	Na_2O/K_2O	B_2O_3	P_2O_5	CaF_2	other
Neopariés®	59.1	6.8/0	19.1/6.8	0/4.3	1.7/1.7	0.6	–	–	–
[37]	57.9	6.9/1.7	20.1/0.8	3.5/0	5.2/0.4	–	–	–	1.2
[40]	52.9	14.0/0.2	20.4/0	0.2/0	5.8/0.2	6.0	–	–	0.24
[45]	60.0	8.0/4.7	18.5/0	4.5/0	6.0/1.1	–	–	–	–
[44]	54.0	2.0/0	42.0/0	–	2.0/0	–	–	–	–
[46]	42.1	–	31.4/0	8.8/0	4.4/0	4.9	3.0	5.4	–

mixing and melting the batch in air using a 100 cm^3 Pt/Rh10 crucible in an electric furnace at 1450 °C for 2 h. The melt was poured onto an iron plate, then crushed and remelted under the same conditions. This refined melt was again poured onto an iron plate. Bubble-free and dark green glasses were obtained. They were then heat-treated for nucleation and crystallization under various conditions. In this study, the crystalline phases precipitated were wollastonite in G3 GC, and wollastonite and spodumene in G5 GC. The glass free from CaF_2 or spodumene showed surface crystallization; however, glasses containing CaF_2 and/or spodumene exhibited bulk crystallization. Properties of GCs sintered at 750 and 950 °C for 10 and 5 h, respectively were studied. The fracture strength of the GCs exhibiting bulk crystallization was two times higher than that of the totally amorphous glasses (Table 4).

Other researchers [44] prepared wollastonite-containing GCs by mixing quartz sand (SiO_2 > 99.5 %) with technically pure $Al(OH)_3$, $CaCO_3$ and Na_2CO_3. The melting of glasses was carried out in 500 ml corundum crucibles at 1500 °C for 2 h. GC samples were obtained by sinter-crystallization of glass powders having size of 75–125 μm. In wollastonite GC containing 2 wt% of Al_2O_3 and 2 wt% of Na_2O the measured coefficient of linear thermal expansion (65 × 10^{-7} K^{-1}) was similar to that of wollastonite (63 × 10^{-7} K^{-1}) and lower compared to the residual glass (73 × 10^{-7} K^{-1}). Wollastonite GCs obtained after 1 h at 950 °C showed a crystallinity value of 56 ± 4 % (Table 4).

Powders of technical-grade silicon oxide (purity >99.5 %) and calcium carbonate (>99.5 %), and reactive-grade H_3BO_3, $4MgCO_3{\cdot}Mg(OH)_2{\cdot}5H_2O$, Na_2CO_3, CaF_2, and $NH_4H_2PO_4$ were used elsewhere [46]. Parent glasses (Table 3) were produced by melting of the batches in Pt crucibles at 1400 °C for 1 h, in air. Glasses in bulk form were produced by casting of melts on preheated bronze moulds and subsequent immediate annealing at 600 °C, close to the glass transition temperature T_g, for 1 h. Bulk glasses were subjected to heat treatment at 700 °C, 800 °C and 900 °C for 1 h. The microstructure of the bulk glasses heat treated at 800 °C (Fig. 5) unequivocally confirmed that the glasses were prone to surface crystallization. Crystal growth advanced towards the core of the bulk glass and, after heat treatment at 900 °C, the crystallization process has been completed (Fig. 5).

The powder of the glass frit was granulated in a 5 vol% polyvinyl alcohol solution in a proportion of 97.5 wt% of frit and 2.5 wt% of PVA. Rectangular bars with dimensions of 4 × 5 × 50 mm^3 were prepared by uniaxial pressing (80 MPa). The bars were sintered at four different temperatures, 700 °C, 750 °C, 800 °C, and 850 °C. The dwelling time at the sintering temperatures was 1 h, while a slow heating rate of 2–3 K. min^{-1} aimed to prevent deformation of the samples. Completely dense samples of dark grey colour but of amorphous nature were obtained at 700 °C, indicating that sintering should precede crystallization (Fig. 6).

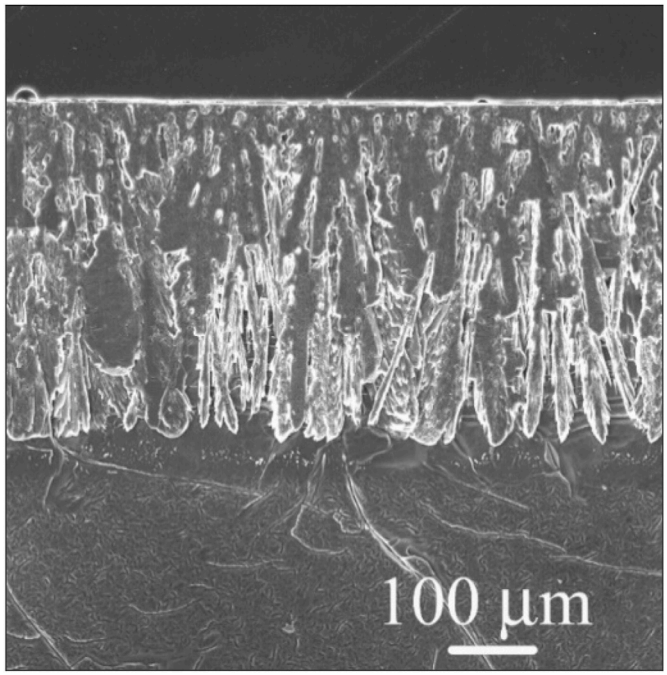

Fig. 5. The microstructure of the bulk glass heat treated at 800 °C [46].

Devitrification starts at higher temperatures. Diopside, wollastonite and akermanite were identified in the X-ray diffractogram after firing at 750 °C (the former two compounds were the dominant phases) (Fig. 6a). The same assemblage of phases was registered in the XRD diffractogram of samples heat-treated at 800 °C. White colour and high degree of densification characterized the samples fired at 750 °C and 800 °C (Fig. 6b). Fig. 7 shows a SEM image of dense sintered GC after heat treatment at 800 °C for 1 h. The measured bending strength, which ranged between 116 and 141 MPa (Table 4), was relatively higher that the values reported for powder-compacts made of glasses of other compositions.

Apparently, there is constant experimentation worldwide on synthesis new wollastonite-containing GCs with improved properties [47–49]. In this regard, selection of the most fusible glass compositions in the wollastonite crystallization field or in the neighbouring regions of $CaO–Al_2O_3–SiO_2$ and $CaO–MgO–SiO_2$ systems may additionally result in significant energy savings.

Table 4
Comparison of mechanical properties of the presented wollastonite-containing GCs with some commercial wollastonite-containing GCs.

	Density ($kg.m^{-3}$)	Flexural strength (MPa)	Modulus of elasticity (GPa)	Mohs hardness/Vickers microhardness	CTE (×10^{-7} K^{-1})
Neopariés® [37,42]	2700	42–44	88 ± 2	6.5/–	57
[37]	2700	55 ± 10	84 ± 2	6.0/–	75
[40]	2600	122	–	–	–
[45]	2657–2710	135–230	–	–	85–90
[44]	2700–2800	76 ± 8	99 ± 2	–	65
[46]	2840–2900	116–141	–	–/4.5–4.6	93–108

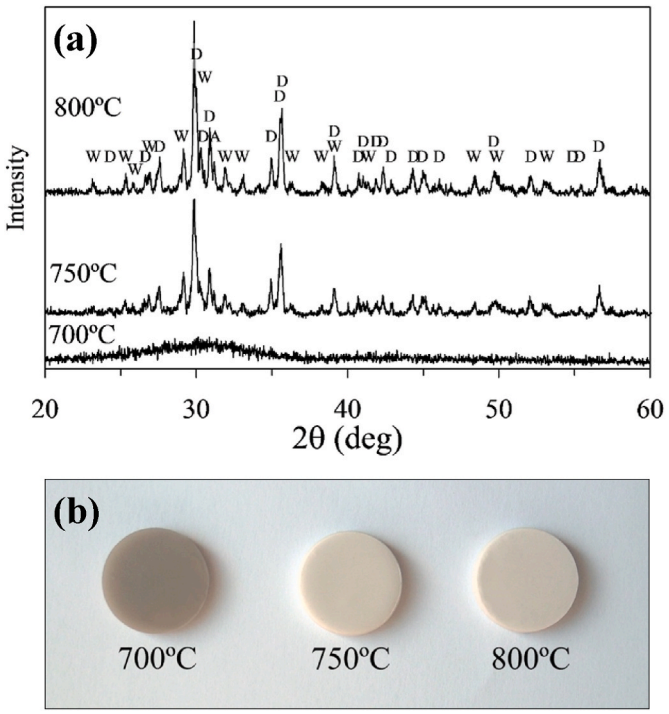

Fig. 6. (a) XRD diffractogram and (b) appearance of sintered glass-powder compacts after heat treatment at 700−800 °C for 1 h [46].

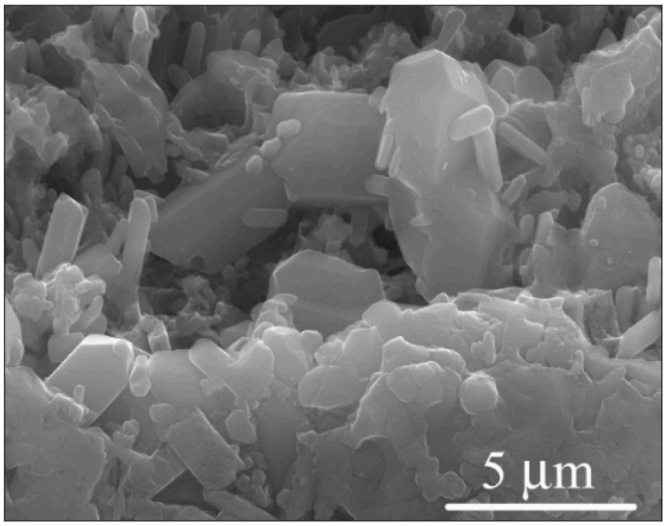

Fig. 7. SEM image of sintered glass-powder compacts after heat treatment at 800 °C for 1 h [46].

5. Biomedical applications of wollastonite-containing glasses/glass-ceramics and composites

In the last 30−40 years, a number of important advances have been made in the domain of bioactive ceramics, glasses, and GCs [50,51]. In particular, wollastonite-containing glasses and GCs in the ternary $CaO–Al_2O_3–SiO_2$ and $CaO–MgO–SiO_2$ systems have gained great interest in biomedical applications owing to their suitable physical, chemical, mechanical, and biological properties [50,52–54]. The high ability to form a surface hydroxyapatite (HA) layer upon contact with the biological fluids [55], which allows bonding with living bone and stimulation of new bone growth, makes these materials very appealing in the field of implantology [50,54,56]. In many cases the interfacial strength of adhesion is equivalent to or even greater than the cohesive strength of bone.

Scientific interest shifted to bioactive GC materials because they can combine the properties of bioactive glass (*i.e.*, high bioactivity) and ceramics of the same composition (*i.e.*, high mechanical properties) [50]. Bromer introduced the concept of bioactive GC material with Ceravital® ($Na_2O–K_2O–MgO–CaO–SiO_2–P_2O_5$) in 1973 [57] followed by Kokubo et al. [58] who developed a bioactive apatite-wollastonite (A-W) GC in the $MgO–CaO–SiO_2–P_2O_5$ system commercially known as Cerabone® A-W GC with (composition (in wt.%): 4.6 MgO, 44.7 CaO, 34.0 SiO_2, 16.2 P_2O_5, and 0.5 CaF_2). This bioactive wollastonite-containing GC exhibits excellent mechanical properties such as bending strength of 220 MPa, indentation fracture toughness of 2.0 ± 0.1 MPa.$m^{0.5}$, modulus of elasticity of 117 GPa [58] and has been found to be capable of forming a strong chemical bond with bone tissue. More specifically, the new GC showed tight bonding to bone comparable with dense hydroxyapatite, and in 25 weeks its load was 70 % of that of bone tissue [59]. Since then, many research groups have been engaged in the study of Cerabone® A-W GCs, performing both *in-vitro* and *in-vivo* studies [60–63]. These GCs were also tested in combination or mixed with other biomaterials; in this regard, Shinzato et al. [61] developed a new bioactive bone cement consisting of PMMA as an organic matrix and wollastonite-containing GC (AW-GC, 4.6 MgO, 44.7 CaO, 34.0 SiO_2, 16.2 P_2O_5, and 0.5 CaF_2) beads as an inorganic filler.

The tensile strength and modulus of elasticity of bioactive and osteoconductive Cerabone® A-W GCs, 220 MPa and 117 GPa, respectively, open new fields of application in biomedicine to these materials. As shown in Table 5, the A–W GCs remain the preference of the clinicians as compared to other commercially available bioactive GCs, exhibiting improved mechanical properties, including high flexural strength, modulus of elasticity, and indentation fracture toughness. More specifically, according to Soares et al. [63], Cerabone® A-W GCs have been successfully used in more than 60,000 clinical cases, including iliac crest vertebral replacement and repair, osseous defect filling and dentistry. However, despite several advantages, Cerabone® A-W GCs demonstrate the lack of bioresorbability in physiological fluids that limits the bone growth rate into the inter-particle spaces. Indeed, the percentage of bone growth into the bone defect after 12 weeks for Cerabone® A-W GCs was shown to be less than 30 % while for 45S5 Bioglass® was higher than 40 % [64]. Therefore, new attempts were undertaken by other research groups to overcome such drawbacks.

Sintering and crystallization of the parent glass in powder compact form, rather than in bulk form (which led to the occurrence of large cracks in the crystallized product), is the most common route to produce wollastonite GCs due to the formation of a crack-free dense crystallized product (due to uniform precipitation of both apatite and wollastonite fine crystals throughout the glass article) [58,63,65]. Thus, bioactive dense GCs based on the $CaO–SiO_2–MgO–Na_2O–Li_2O$ system were developed from glass powder compacts by Soares et al. [63] via sinter-crystallization process at different temperatures (800−1000 °C). Four glass compositions were formulated by a proprietary software (Reformix) and tested by changing mainly the calcium content (from 20 to 40 mol%) and the minor components: alumina, zirconia and zinc oxide. Wollastonite-diopside-combeite GCs showed the best results, *i.e.*, flexural strength of 98 ± 7 MPa, hardness of 5.5 ± 0.5 GPa, were not cytotoxic, and demonstrated promising in vitro bioactivity, suggesting these GCs as candidates for bone grafts. The authors concluded that the addition of ZrO_2 or Al_2O_3 or a high CaO content (~40 mol%) promote the sintering process, however in turn bioactivity tended to decrease due to densification/surface area reduction.

Aiming at improving mechanical properties of wollastonite GCs, TiO_2 nanofibers were introduced to high-purity wollastonite in the amount of 0, 10, 20 and 30 wt%. and then composites were sintered at 900, 1100 and 1250 °C. In general, it was demonstrated that addition of TiO_2 nanofibers strongly enhanced the compressive strength (~6–60 MPa), and microhardness (~5–27 GPa). Moreover, both wollastonite

Table 5
Comparison of mechanical properties of the presented wollastonite-containing GCs [52,56,63,66–69,72,74,75,77–79,82] with the corresponding values of the human natural tissues [52], and commercial wollastonite-containing GC [57,85].

	Flexural strength (MPa)	Modulus of elasticity (GPa)	Comp. strength (MPa)	Micro-hardness (GPa)	Indent. fracture toughness (MPa.m$^{0.5}$)	Bio-activity	Bonding strength to bone	Proposed application
Properties of natural tissues [52]								
HA	60–120	–	100–150	0.09–0.14	0.8–1.2	–	–	–
Dentine	230–305	15–30	–	<0.6	3	–	–	–
Cortical Bone	50–150	7–30	100–135	0.06–0.07	2–12	–	–	–
Trabecular Bone	10–20	0.05–0.5	1.5–7.5	0.5–1	0.7–1.1	–	–	–
Commercially Available GCs [57,85]								
A-W GC (Cerabone®)	220	117	–	6.9 ± 0.3	2.0 ± 0.1	V	<1 MPa	Biomedical applications
Bioverit I	140–180	70–88	500	5	1.2–2.1	V	2.3 MPa	Bone substitutes
Bioverit II	90–140	70	450	~8	1.2–1.8	V	–	Bone substitutes
Biosilicate	210	60–80	–	–	1	V	–	Bone regeneration
Ceravital	100–150	–	500	–	–	V	–	Orthopaedics
Wollastonite-containing GCs and proposed biomedical applications								
[52,56]	–	27–34	–	6.0–6.7	2.1–2.6	V	–	Dental Implants
[63]	98 ± 7	–	–	5.5 ± 0.5	–	V	–	Bone graft implants
[66]	–	–	~6–60	~5–27	–	V	–	Bone substitute
[67]	–	–	–	–	–	V	–	Biomedical applications
[68]	–	–	225	0.067	–	–	–	Biomedical applications
[69,70]	–	89–100	–	–	4.6–5.6	V	–	Dental Implants
[72]	–	–	3.9–4.7	–	–	–	–	Bone tissue engineering
[74]	–	0.308–0.436	2.8–3.5	–	–	V	–	Bone substitute
[75]	–	0.225–0.250	12.5–15	–	–	–	–	Biomedical applications
[77,78]	–	–	29.7	1.4	–	V	–	Load-bearing applications
[79]	–	14.5–18.1	–	–	–	V	–	Implant applications
[82]	–	1.2–5.4 2.2–6.5	37–56 62–77	–	–	V	–	Dental implants

and wollastonite/TiO_2 nanofibers showed good bioactivity after 1, 7, 14, and 30 days of storage in SBF at 36.5 °C. Based on the promising results of this study, the authors concluded that TiO_2 nanofibers enable wollastonite GCs as promising candidates for bone graft substitutes in high-load-bearing sites [66].

Silver-doped (AgO, 2, 4 and 6 mol%) wollastonite GCs were successfully prepared by Palakurthy et al. [67] using the sol-gel method. According to their results, the addition of AgO (a) decreases the degradation rate of wollastonite, (b) results in the enhancement of apatite layer development on the surface of the samples, and (c) allows forming an excellent inhibition zone of pathogens such as *E. coli* and *S. aureus* as compared to the pure form of wollastonite. Consequently, Ag-doped wollastonite GCs are potentially multifunctional biomaterials that may find applications in the biomedical domain.

Mansoor and Dasharath [68], through spark plasma sintering (SPS) technology, produced dense specimens using $CaSiO_3$ ceramic powder in addition of TiO_2 and HA composites. The dense $CaSiO_3$/TiO_2/HA ceramic composite heat-treated at 1250 °C exhibited the relative density 98.8 %, Vickers hardness 67 MPa, and compressive strength 225 MPa, which open new horizons for biomedical applications as the above values ranged very close to the corresponding values of cortical bone (Table 5).

Wollastonite-containing GCs have attracted the interest of researchers for dental applications as well. Saadaldin et al. [69,70], developed glasses in SiO_2–Al_2O_3–CaO–CaF_2 system in order to synthesize machinable wollastonite GCs with mechanical properties suitable for dental implant applications. The wollastonite was the main crystalline phase in the high strength, chemically durable and machinable sintered GCs. The mechanical properties (modulus of elasticity of 89–100 GPa, true hardness 4.85–5.17 GPa and indentation fracture toughness 4.62–5.58 MPa.m$^{0.5}$ [69]) and biological behaviour (bioactivity and biocompatibility [70]) of wollastonite-containing GCs make these materials as appealing options for immediate non-metallic one-piece dental implant applications as alternative to currently-avaialable commercial dental implants. Novel compositions based on the CaO–MgO–SiO_2 ternary system, with the additions of Na_2O, K_2O, P_2O_5, CaF_2, and Al_2O_3, were developed by Dimitriadis et al. [52,56] in order to produce GCs for dental implant applications. Bioactive dense GCs, produced by sintering and controlled crystallization of glass-powder compacts, exhibited mechanical properties better than those of the titanium and zirconia dental implant materials used as references, and their modulus of elasticity (27–34 GPa), microhardness (6.0–6.7 GPa), and indentation fracture toughness (2.1–2.6 MPa.m$^{0.5}$) were comparable to those of human jaw bone and dentine (Table 5) classifying these materials as candidates for dental implant applications.

Porous wollastonite-containing bioceramics with controllable biodegradation rate and appreciable mechanical strength were thought to be the promising candidates for bone regenerative biomedicine [71]. Elsayed et al. [72] fabricated scaffolds from wollastonite-diopside GCs using 3D-printing technology followed by heat treatment at 1100 °C; the sintered porous samples exhibited high compressive strength (3.9−4.7 MPa) considering the large porosity (67−76 vol%). These highly porous wollastonite-diopside GCs show promise for use in bone tissue engineering. Barbosa et al. [73] developed wollastonite/β-TCP porous ceramic scaffolds by the polymer sponge replication. According to their results the wollastonite/β-TCP porous structure is bioactive and osteoconductive, excellent for permeation and adhesion of cells as well as flowing in/out of nutrients and residues. In vivo experiments showed that the investigated materials provided biocompatibility and promoted bone formation, stimulating the process of bone repair in rabbits. Novel porous bio-nanocomposite scaffolds made of hydroxyapatite-wollastonite reinforced with 0, 5, 10, and 15 wt%

alumina nanoparticles in the range of 40–80 nm (HA/WS/ALN) were studied by Aghdam et al. [74]. The porous cylindrical specimens after sintering at 800–850 °C showed density of 1960–2900 $kg.m^{-3}$, compressive strength of 2.8–3.5 MPa, elastic modulus of 308–436 MPa, and porosity 49−61 %. The values of compressive strength and elastic modulus are very close to the corresponding values of trabecular bone (Table 5). Finally, the combination of mechanical and biological analysis showed that the specimens with 10 wt% alumina nanoparticles had both proper compression strength (2.95 MPa) vs. porosity percentage (58 %) and bioactivity response.

In recent years, additive manufacturing has been proposed in the field of bone repair and tissue engineering as a versatile method for fabricating porous bioceramic scaffolds. Shen et al. [75] fabricated porous bioceramics from wollastonite/diopside without and with Zn or Sr doping using additive manufacturing technology (Direct Ink Writing, DIW). According to their experimental results, the presence of high-density micropores had a strong influence on the strength of the scaffolds, *i.e.*, the compressive strength of the specimens containing micropores ranged from 12.5 to 15 MPa, while the compressive strength of the specimens without micropores ranged from 26 to 31 MPa and the modulus of elasticity of the specimens with micropores was determined to be 225–250 MPa. These values are close to the corresponding ranges for trabecular bone (Table 5). Regarding biodegradability, it was found that Zn or Sr doping may slightly affect the biodegradation rate of the porous bioceramics. Another group of researchers [76] fabricated 6 % Mg-substituted wollastonite porous bioactive scaffolds using AM technology, *i.e.*, 3D stereolithography, which opens up opportunities for developing scaffolds with tailored pore architecture. The developed porous scaffolds with precisely controlled pore dimensions showed appreciable mechanical strength, bioactivity, and neo-bone ingrowth. Particularly, according to their conclusion, "*Mg substitution in wollastonite can contribute to a significant enhancement of mechanical properties*".

Bioactive glass with composition (in wt.%) 46.1 SiO_2, 28.7 CaO, 8.8 MgO, 6.2 P_2O_5, 5.7 CaF_2, 4.5 Na_2O [77] was used to prepare porous wollastonite-containing GC scaffolds upon high-temperature thermal treatment [78]. The glass powder underwent sinter-crystallization, leading to consolidation of the scaffold structure and concurrent development of three biocompatible crystalline phases, *i.e.*, diopside, wollastonite and fluorapatite. The scaffolds exhibited a 3D pore–strut architecture and total porosity (68 vol%) matching those of spongy bone, while the compressive strength (29.7 MPa) and elastic modulus (1.4 GPa) were superior to those of osseous tissue, suggesting suitability for application in load-bearing sites. The scaffolds also exhibited highly promising bioactive properties in vitro, being covered by a calcium phosphate layer after immersion in simulated body fluids for just 48 h (Table 5).

In recent years, research groups have turned to combining bioactive wollastonite-containing GCs with other biocompatible ceramics or alloys to develop a good candidate for implant applications. Ramli et al. [79] investigated the combination of bioactive wollastonite with Ti_6Al_4V alloy for implant applications. According to their results, the highest modulus of elasticity obtained was 18.10 GPa, close to the corresponding values of dentine and cortical bone (Table 5, and the Ti_6Al_4V/wollastonite materials studied were not toxic, as the cell viability test showed that that cell proliferation increased over time. Baino et al. [80] fabricated wollastonite-containing bioceramic coatings on alumina substrates by the airbrush spraying of glass-based materials in the SiO_2–CaO–Na_2O–Al_2O_3 system and subsequent sintering. The adhesion between wollastonite-containing bioceramic coating and alumina substrate was very good after the heat treatment process (at 1000 °C for 3 h), as the calculated bonding strength was 22.3 ± 5.1 MPa (by applying tensile loads), which is higher than the minimum value of 15 MPa recommended in ISO 13779 [81] for HA coatings on surgical implants. The above data suggests their mechanical suitability for biomedical use. Another research group [82] developed bioactive wollastonite and wollastonite-diopside flame-sprayed coatings on stainless steel and titanium implants in order to (a) improve the resistance to corrosion of the metal, (b) increase the bioactivity, and (c) promote mechanical stability by chemical bonding with the bone. Regarding the bioactivity, these coatings demonstrated a good apatite-forming ability in SBF, with a faster dissolution rate of the wollastonite coating. As far as the mechanical performance, Vickers microhardness of 1.2–5.4 and 2.2−6.5 GPa and elastic modulus of 37–56 and 62−77 GPa were reported for wollastonite and wollastonite-diopside coatings, respectively; the mentioned values ranged very close to the cortical bone. Overall, the above-mentioned properties make these bioactive coatings as promising candidate materials for bone and dental implants.

It should be highlighted that, according to a recent retrospective study on 99 patients collectively bearing 117 hip joint prostheses [83], the use of apatite-wollastonite GC is clinically working very well as a coating on the acetabular cup or stem of the implant in total hip arthroplasty.

A wollastonite-containing GC produced by sinter-crystallization of SiO_2–CaO–Na_2O–Al_2O_3 glass powders was also proposed for restorative dentistry (artificial dental crown) due to its favourable aesthetic properties (whiteness), biochemical inertness and high indentation fracture toughness, which was three times higher than that of enamel [84].

Yet Cerabone® A-W GCs remains as the model to be emulated, recently new bioactive wollastonite-containing GCs and wollastonite-containing composites were synthesized, and their properties are discussed elsewhere [27,86–92]. Indeed, there are big challenges to overcome drawbacks of Cerabone® A-W GCs considering, for instance, the fact that bone growth into the bone defect for Cerabone® A-W GCs into the bone defect after 12 weeks is only 30 %. Moreover, the long-term results of primary total hip arthroplasty using a bioactive bone cement containing apatite-wollastonite GC powder were shown to be unsatisfactory [93].

6. Major challenges and future perspectives

Wollastonite has been investigated and proposed for decades in many fields of application, ranging from thermal insulation to automotive industry. A plenty of methods have been patented and implemented at the industrial scale to fabricate pure wollastonite commercial products, as reviewed elsewhere [9]. However, there are still some important challenges related to the development of wollastonite-containing GCs, which are briefly outlined below.

The design of crystal micro- or even nano-structure is of utmost importance in GC materials because these characteristics dictate most performances of the final material, like mechanical properties. Comprehensive knowledge of toughening mechanisms, for example, is a primary step for developing tough, strong, and durable GCs. In this regard, the wollastonite crystal morphology, size, shape and volume fraction embedded in the residual glass matrix are all very important parameters that can be modulated and tailored at the micro/nano-scale by properly designing the composition of the parent glass as well as the subsequent thermal treatments (*e.g.*, sintering process that may take place concurrently to crystallization). An interesting example of microstructural design for increasing the flexural strength of GCs was reported by Faeghi-Nia et al., who induced the crystallization of wollastonite crystals in the vicinity of mica crystals in materials encompassing different crystalline phases, thus creating interfacial compressive stresses promoted by expansion mismatch [94].

Experimental optimization of GCs is what is commonly carried out, although in general this does not guarantee to truly achieve the desired properties. On the contrary, modelling-based approaches begin to be used in academia and industry as they allow a reliable optimization of glasses and GCs to be achieved [95,96]. Although computational cost still remains quite high, machine learning strategies yielded promising results in applications like prediction of elastic modulus and crystal growth/nucleation [97]. In those cases where there is a strong

dependency on viscosity, machine learning models are also useful to overcome the need for experimental viscosimetric measurements.

As regards the production method, sinter-crystallization of melt-derived glass powder compacts is the easiest and most popular approach for producing wollastonite-containing GCs. An alternative approach relies on applying the sol-gel method, which on one hand is more complicated and time-consuming than melting routes but, on the other hand, allows obtaining materials with special features (*e.g.*, mesoporosity, nanoparticulate systems etc.). It cannot be ignored, however, that wet-chemistry methods addressed to synthesize such GC products typically require organic solvents and chemicals like acids, bases, ethanol, tetraethyl orthosilicate (TEOS) and calcium nitrate which are dangerous to health and environment. Development of "greener" aqueous syntheses using water as the unique eco-friendly solvent would deserve further investigation in the future.

Lastly, we would like to emphasize that some novel applications of wollastonite-containing GCs have emerged over the last few years and deserve to be further explored. An interesting example comes from the field of biomedical devices: while wollastonite-containing GCs are typically used for bone/dental repair because of the physical and mechanical affinity with hard tissues, macroporous implants from the sinter-crystallization of SiO_2–Na_2O–CaO–Al_2O_3 glass powder were shown to exhibit highly favourable properties as ocular biomaterials for globe replacement after enucleation [98,99]. Specifically, the surface roughness and related physical characteristics were similar to those of porous polyethylene and alumina that are the today's preferred devices by orbital surgeons [100,101].

7. Conclusions

This review offers a comprehensive overview of wollastonite-containing GCs, including their crystallization behaviour, notable mechanical and biological properties, and commercial applications. The following conclusions have been drawn from the study:

- Generally, the advantages of designing GCs containing wollastonite crystals in the CaO–Al_2O_3–SiO_2 and CaO–MgO–SiO_2 systems are simpler fabrication, improvement of mechanical properties and a wide range of applications.
- The most fusible eutectic in the CaO–MgO–SiO_2 system is formed between wollastonite, diopside and tridymite with a melting point of 1320 °C. While the most fusible eutectics in the CaO–Al_2O_3–SiO_2 system with melting points 1165, 1265 and 1307 °C is adjacent to the fields of a wollastonite, anorthite and gehlenite crystallization. The selection of the most fusible glass compositions may result into significant energy savings.
- The production of the wollastonite-containing GCs for construction and architectural application satisfies the requirements for environmental protection as the starting glass is produced from wastes or recycled by-products.
- In the CaO–MgO–SiO_2 ternary system, the most common method for producing wollastonite-containing GCs is through the sintering and crystallization of the parent glass in powder compact form, rather than in bulk form. This approach ensures the formation of a crack-free dense crystallized product.
- Incorporating wollastonite crystals in close proximity to other crystals, such as diopside, within GCs is a strategic method for achieving a fine microstructure and enhancing the mechanical properties of the resulting materials.
- The mechanical properties and biological behaviour, including bioactivity and biocompatibility, of wollastonite-containing GCs make them highly attractive for immediate non-metallic dental implant applications.
- Despite its excellent mechanical properties and ability to form a strong chemical bond with bone tissue, Cerabone® A-W glass-ceramic (GC) has limitations in its application. This material lacks bioresorption in physiological fluids, which hinders the rate of bone growth in the inter-particle spaces.

Declaration of competing interest

The authors declare that they have no known competing financial interests or personal relationships that could have appeared to influence the work reported in this paper.

Acknowledgments

HRF thank CICECO-Aveiro Institute of Materials, UIDB/50011/2020, UIDP/50011/2020 & LA/P/0006/2020, financed by national funds through the FCT/MCTES (PIDDAC).

References

[1] J.W. Anthony, R.A. Bideaux, W. Bladh, K.M.C. Nichols, Handbook of Mineralogy: Silica, Silicates, first ed., Mineral Data Publishing, Tucson, 1995.
[2] Y. Tian, G.D. Li, J.S. Chen, Chemical formation of mononuclear univalent zinc in a microporous crystalline silicoaluminophosphate, J. Am. Chem. Soc. 125 (2003) 6622–6623, https://doi.org/10.1021/ja0343757.
[3] D. Sun, L. Sun, M. Luo, Z. Gou, One-pot preparation of 3-hydroxymethyl 2,5-diketopiperazine for total synthesis of peticinnamin E, Asian J. Chem. 23 (2011) 5169–5170.
[4] S.A. Solin, Clays and clay intercalation compounds: properties and physical phenomena, Annu. Rev. Mater. Sci. 27 (1997) 89–115, https://doi.org/10.1146/annurev.matsci.27.1.89.
[5] D.U. Tulyaganov, F. Baino, in: F. Baino, M. Tomalino, D.U. Tulyaganov (Eds.), Silicate Glasses and Glass-Ceramics: Types, Role of Composition and Processing Methods, Ceram. Glas. Glas, PoliTO Springer Series. Springer, 2021, pp. 119–152, https://doi.org/10.1007/978-3-030-85776-9_4.
[6] D. Sani, G. Moriconi, G. Fava, V. Corinaldesi, Leaching and mechanical behaviour of concrete manufactured with recycled aggregates, Waste Manag. 25 (2005) 177–182, https://doi.org/10.1016/j.wasman.2004.12.006.
[7] A. Telesca, M. Marroccoli, D. Calabrese, G.L. Valenti, F. Montagnaro, Flue gas desulfurization gypsum and coal fly ash as basic components of prefabricated building materials, Waste Manag. 33 (2013) 628–633, https://doi.org/10.1016/j.wasman.2012.10.022.
[8] C. Wu, J. Chang, W. Fan, Bioactive mesoporous calcium-silicate nanoparticles with excellent mineralization ability, osteostimulation, drug-delivery and antibacterial properties for filling apex roots of teeth, J. Mater. Chem. 22 (2012) 16801–16809, https://doi.org/10.1039/c2jm33387b.
[9] N.I. Demidenko, L.I. Podzorova, V.S. Rozanova, V.A. Skorokhodov, V. Y. Shevchenko, Wollastonite as a new kind of natural material (a review), Glas, Ceram. (English Transl. Steklo i Keramika). 58 (2001) 308–311.
[10] G.A. Khater, A. Abdel-Motelib, A.W. El Manawi, M.O. Abu Safiah, Glass-ceramics materials from basaltic rocks and some industrial waste, J. Non-Cryst. Solids 358 (2012) 1128–1134, https://doi.org/10.1016/j.jnoncrysol.2012.02.010.
[11] C.J. Jeon, E.S. Kim, J.H. Cho, Effects of crystallization behaviour on microwave dielectric properties of $(Ca_{1-x}Mg_x)SiO_3$ glass-ceramics, Mater. Res. Bull. 96 (2017) 60–65, https://doi.org/10.1016/j.materresbull.2017.01.042.
[12] D. He, C. Gao, Effect of boron on crystallization, microstructure and dielectric properties of CBS glass-ceramics, Ceram. Int. 44 (2018) 16246–16255, https://doi.org/10.1016/j.ceramint.2018.06.011.
[13] Y. Hou, Y. Wang, G.H. Zhang, K.C. Chou, Preparation of fully dense and magnetically controllable $CaO-Al_2O_3-SiO_2-Na_2O-Fe_3O_4$ glass ceramics by hot pressing, J. Eur. Ceram. Soc. 41 (2021) 5201–5213, https://doi.org/10.1016/j.jeurceramsoc.2021.04.024.
[14] K.A. Almasri, H.A.A. Sidek, K.A. Matori, M.H.M. Zaid, Effect of sintering temperature on physical, structural and optical properties of wollastonite based glass-ceramic derived from waste soda lime silica glasses, Results Phys. 7 (2017) 2242–2247, https://doi.org/10.1016/j.rinp.2017.04.022.
[15] B. Zhang, Y. Yu, L. Guo, S. Kang, Y. Cheng, Z. Yan, L. Wang, Microstructure evolution of CMAS glass below melting temperature and its potential influence on thermal barrier coatings, Ceram. Int. 48 (2022) 32877–32885, https://doi.org/10.1016/j.ceramint.2022.07.215.
[16] G.-Y. Hung, P.-Y. Chen, C.-S. Chen, J.-Y. Qiu, C.-S. Tu, K.-C. Feng, Tailoring microwave-millimeter-wave dielectric and mechanical properties in $CaO-SiO_2$ glass-ceramics by P_2O_5 nucleating agent, Ceram. Int. (2023), https://doi.org/10.1016/j.ceramint.2023.06.091.
[17] E.F. Osborn, A. Muan, Phase Equilibria Diagrams of Oxide Systems, American Ceramic Society with the Edward Orton Jr. Ceramic Foundation, Columbus, Ohio, 1960.
[18] M. Tomalino, in: F. Baino, M. Tomalino, D.U. Tulyaganov (Eds.), Mineralogy and Properties of Raw Materials and Crystalline Phases of Ceramics and Glass-Ceramics, Ceram. Glas. Glas., Springer International Publishing, Cham, 2021, pp. 47–74.
[19] C. Klein, B. Dutrow, Manual of Mineral Science, 23rd ed., Wiley, New Jersey, 2007.

[20] R.M. Thompson, X. Xie, S. Zhai, R.T. Downs, H. Yang, A comparison of the $Ca_3(PO_4)_2$ and $CaSiO_3$ systems, with a new structure refinement of tuite synthesized at 15 GPa and 1300 °c, Am. Mineral. 98 (2013) 1585–1592, https://doi.org/10.2138/am.2013.4435.

[21] R. Shamsudin, H. Ismail, M. Azmi, A. Hamid, R. Awang, Characteristics of wollastonite synthesized from rice husk and rice straw, Solid State Sci. Technol. 24 (2016) 61–69.

[22] J. Vázquez, C. Wagner, P. Villares, R. Jiménez-Garay, Glass transition and crystallization kinetics in $Sb_{0.18}As_{0.34}Se_{0.48}$ glassy alloy by using non-isothermal techniques, J. Non-Cryst. Solids 235–237 (1998) 548–553.

[23] C.G. Zenebe, A review on the role of wollastonite biomaterial in bone tissue engineering, BioMed Res. Int. 2022 (2022), https://doi.org/10.1155/2022/4996530.

[24] A. Gian, Study on Ultraviolet-A of $CaSiO_3$: Ce^{3+} Film Phosphor, Pukyong National University, 2020.

[25] National Minerals Information Center, Wollastonite, 2003.

[26] S.S. Hossain, P.K. Roy, Study of physical and dielectric properties of bio-waste-derived synthetic wollastonite, J. Asian Ceram. Soc. 6 (2018) 289–298, https://doi.org/10.1080/21870764.2018.1508549.

[27] S.S. Hossain, S. Yadav, S. Majumdar, S. Krishnamurthy, R. Pyare, P.K. Roy, A comparative study of physico-mechanical, bioactivity and hemolysis properties of pseudo-wollastonite and wollastonite glass-ceramic synthesized from solid wastes, Ceram. Int. 46 (2020) 833–843, https://doi.org/10.1016/j.ceramint.2019.09.039.

[28] S. Vichaphund, M. Kitiwan, D. Atong, P. Thavorniti, Microwave synthesis of wollastonite powder from eggshells, J. Eur. Ceram. Soc. 31 (2011) 2435–2440, https://doi.org/10.1016/j.jeurceramsoc.2011.02.026.

[29] A. Yazdani, H.R. Rezaie, H. Ghassai, Investigation of hydrothermal synthesis of wollastonite using silica and nano silica at different pressures, J. Ceram. Process. Res. 11 (2010) 348–353.

[30] G.M. Azarov, E. V Maiorova, M.A. Oborina, A. V Belyakov, Wollastonite raw materials and their applications (a review), Glas, Ceram 52 (1995) 13–16.

[31] M.J. Ribeiro, D. Tulyaganov, Traditional ceramics manufacturing, in: Ceram. Glas. Glas., Springer International Publishing, Cham, 2021, pp. 75–119, https://doi.org/10.1007/978-3-030-85776-9_4.

[32] M.C. Day, F.C. Hawthorne, A structure hierarchy for silicate minerals: chain, ribbon, and tube silicates, Mineral. Mag. 84 (2020) 165–244, https://doi.org/10.1180/mgm.2020.13.

[33] J.E. Ricci, Data of Geochemistry, sixth ed., United States Government Printing Office, Washington, DC, 1965.

[34] J. Ferguson, H. Merwin, The ternary system $CaO-MgO-SiO_2$, Proc. Natl. Acad. Sci. U. S. A. 5 (1919) 16–18, https://doi.org/10.1073/pnas.5.1.16.

[35] D.U. Tulyaganov, K. Dimitriadis, S. Agathopoulos, H.R. Fernandes, Glasses and glass-ceramics in the CaO–MgO–SiO_2 system: diopside containing compositions - a brief review, J. Non-Cryst. Solids 612 (2023), 122351, https://doi.org/10.1016/j.jnoncrysol.2023.122351.

[36] S.R. Teixeira, R.S. Magalhães, A. Arenales, A.E. Souza, M. Romero, J.M. Rincón, Valorization of sugarcane bagasse ash: producing glass-ceramic materials, J. Environ. Manag. 134 (2014) 15–19, https://doi.org/10.1016/j.jenvman.2013.12.029.

[37] A. Karamanov, I. Penkov, B. Bogdanov, Diopside marble-like sintered glass-ceramics, Glass Sci. Technol. IIternational J. Ger. Soc. Glass Technol. 67 (1994) 202–206.

[38] A. Karamanov, M. Pelino, M. Salvo, I. Metekovits, Sintered glass-ceramics from incinerator fly ashes. Part II. The influence of the particle size and heat-treatment on the properties, J. Eur. Ceram. Soc. 23 (2003) 1609–1615, https://doi.org/10.1016/S0955-2219(02)00371-0.

[39] E. Montoya-Quesada, M.A. Villaquirán-Caicedo, R.M. De Gutiérrez, New glass-ceramic from ternary-quaternary mixtures based on Colombian industrial wastes: blast furnace slag, cupper slag, fly ash and glass cullet, Bol. La Soc. Esp. Ceram. y Vidr. 61 (2022) 284–299, https://doi.org/10.1016/j.bsecv.2020.11.009.

[40] M.I. Martín, F.A. López, F.J. Alguacil, M. Romero, Technical characterization of sintered-glass ceramics derived from glass fibers recovered by pyrolysis, J. Mater. Civ. Eng. 27 (2015), https://doi.org/10.1061/(asce)mt.1943-5533.0001090.

[41] G.A. Khater, Diopside-anorthite-wollastonite glass-ceramics based on waste from granite quarries, Glas, Technol. 51 (2010) 6–12.

[42] S. Nakamura, Crystallized Glass Article Having a Surface Pattern, 1976, 3955989.

[43] Electric Glass Building Materials Co.,Ltd (n.d.), http://www.neg.co.jp/arch/.

[44] A. Karamanov, M. Pelino, Induced crystallization porosity and properties of sintereds diopside and wollastonite glass-ceramics, J. Eur. Ceram. Soc. 28 (2008) 555–562, https://doi.org/10.1016/j.jeurceramsoc.2007.08.001.

[45] E. Waraporn, M. Shigeki, Preparation of glass-ceramics using fly ash as a raw material, J. Sci. Technol. 13 (2005) 137–142.

[46] D.U. Tulyaganov, S. Agathopoulos, J.M. Ventura, M.A. Karakassides, O. Fabrichnaya, J.M.F. Ferreira, Synthesis of glass-ceramics in the $CaO-MgO-SiO_2$ system with B_2O_3, P_2O_5, Na_2O and CaF_2 additives, J. Eur. Ceram. Soc. 26 (2006) 1463–1471, https://doi.org/10.1016/j.jeurceramsoc.2005.02.009.

[47] Y. Luo, S. Bao, Y. Zhang, Recycling of granite powder and waste marble produced from stone processing for the preparation of architectural glass-ceramic, Construct. Build. Mater. 346 (2022), 128408, https://doi.org/10.1016/j.conbuildmat.2022.128408.

[48] L. Deng, F. Yun, R. Jia, H. Li, X. Jia, Y. Shi, X. Zhang, Effect of SiO_2/MgO ratio on the crystallization behavior, structure, and properties of wollastonite-augite glass-ceramics derived from stainless steel slag, Mater. Chem. Phys. 239 (2020), 122039, https://doi.org/10.1016/j.matchemphys.2019.122039.

[49] P. Alfonso, O. Tomasa, M. Garcia-Valles, M. Tarrago, S. Martínez, Glass-ceramic crystallization from tailings of the Morille tungsten deposit, Spain, Mater. Lett. 312 (2022), 131694, https://doi.org/10.1016/j.matlet.2022.131694.

[50] H.R. Fernandes, A. Gaddam, A. Rebelo, D. Brazete, G.E. Stan, J.M.F. Ferreira, Bioactive glasses and glass-ceramics for healthcare applications in bone regeneration and tissue engineering, Materials 11 (2018) 1–54, https://doi.org/10.3390/ma11122530.

[51] S.M. Best, A.E. Porter, E.S. Thian, J. Huang, Bioceramics: past, present and for the future, J. Eur. Ceram. Soc. 28 (2008) 1319–1327, https://doi.org/10.1016/j.jeurceramsoc.2007.12.001.

[52] K. Dimitriadis, D.U. Tulyaganov, S. Agathopoulos, Development of novel alumina-containing bioactive glass-ceramics in the $CaO-MgO-SiO_2$ system as candidates for dental implant applications, J. Eur. Ceram. Soc. 41 (2021) 929–940, https://doi.org/10.1016/j.jeurceramsoc.2020.08.005.

[53] N. Keyvani, V.K. Marghussian, H.R. Rezaie, M. Kord, Effect of Al_2O_3 content on crystallization behavior, microstructure, and mechanical properties of $SiO_2-Al_2O_3-CaO-MgO$ glass-ceramics, Int. J. Appl. Ceram. Technol. 8 (2011) 203–213, https://doi.org/10.1111/j.1744-7402.2009.02428.x.

[54] D.U. Tulyaganov, M.E. Makhkamov, A. Urazbaev, A. Goel, J.M.F. Ferreira, Synthesis, processing and characterization of a bioactive glass composition for bone regeneration, Ceram. Int. 39 (2013) 2519–2526, https://doi.org/10.1016/j.ceramint.2012.09.011.

[55] X. Liu, C. Ding, P.K. Chu, Mechanism of apatite formation on wollastonite coatings in simulated body fluids, Biomaterials 25 (2004) 1755–1761, https://doi.org/10.1016/j.biomaterials.2003.08.024.

[56] K. Dimitriadis, D. Moschovas, D.U. Tulyaganov, S. Agathopoulos, Development of novel bioactive glass-ceramics in the $Na_2O/K_2O-CaO-MgO-SiO_2-P_2O_5-CaF_2$ system, J. Non-Cryst. Solids 533 (2020), 119936, https://doi.org/10.1016/j.jnoncrysol.2020.119936.

[57] M. Montazerian, E. Dutra Zanotto, History and trends of bioactive glass-ceramics, J. Biomed. Mater. Res., Part A 104 (2016) 1231–1249, https://doi.org/10.1002/jbm.a.35639.

[58] T. Kokubo, S. Ito, M. Shigematsu, S. Sakka, T. Yamamuro, Mechanical properties of a new type of apatite-containing glass-ceramic for prosthetic application, J. Mater. Sci. 20 (1985) 2001–2004, https://doi.org/10.1007/BF01112282.

[59] T. Nakamura, T. Yamamuro, S. Higashi, T. Kokubo, S. Itoo, A new glass-ceramic for bone replacement: evaluation of its bonding to bone tissue, J. Biomed. Mater. Res. 19 (1985) 685–698, https://doi.org/10.1002/jbm.820190608.

[60] T. Duminis, S. Shahid, R.G. Hill, Apatite glass-ceramics: a review, Front. Mater. 3 (2017) 1–15, https://doi.org/10.3389/fmats.2016.00059.

[61] Shuichi Shinzato, M. Kobayashi, W.F. Mousa, M. Kamimura, M. Neo, Y. Kitamura, T. Kokubo, T. Nakamura, Bioactive polymethyl methacrylate-based bone cement Comparison of glass beads, apatite- and wollastonite-containing glass-ceramic, and hydroxyapatite fillers on mechanical and biological properties, J. Biomed. Mater. Res. 51 (2000) 258–272, https://doi.org/10.1002/(SICI)1097-4636(200008)51:2<258::AID-JBM15>3.0.CO;2-S.

[62] E.D. Zanotto, A bright future for glass-ceramics, Am. Ceram. Soc. Bull. 89 (2010) 19–27.

[63] V.O. Soares, J.K.M.B. Daguano, C.B. Lombello, O.S. Bianchin, L.M.G. Gonçalves, E.D. Zanotto, New sintered wollastonite glass-ceramic for biomedical applications, Ceram. Int. 44 (2018) 20019–20027, https://doi.org/10.1016/j.ceramint.2018.07.275.

[64] E. Fiume, J. Barberi, E. Verné, F. Baino, Bioactive glasses: from parent 45S5 composition to scaffold-assisted tissue-healing therapies, J. Funct. Biomater. 9 (2018) 24, https://doi.org/10.3390/jfb9010024.

[65] T. Kokubo, S. Ito, S. Sakka, T. Yamamuro, Formation of a high-strength bioactive glass-ceramic in the system $MgO-CaO-SiO_2-P_2O_5$, J. Mater. Sci. 21 (1986) 536–540, https://doi.org/10.1007/BF01145520.

[66] I.H.M. Aly, L. Abed Alrahim Mohammed, S. Al-Meer, K. Elsaid, N.A.M. Barakat, Preparation and characterization of wollastonite/titanium oxide nanofiber bioceramic composite as a future implant material, Ceram. Int. 42 (2016) 11525–11534, https://doi.org/10.1016/j.ceramint.2016.02.060.

[67] S. Palakurthy, A.A. P, V.R. K, In vitro evaluation of silver doped wollastonite synthesized from natural waste for biomedical applications, Ceram. Int. 45 (2019) 25044–25051, https://doi.org/10.1016/j.ceramint.2019.03.169.

[68] P. Mansoor, S.M. Dasharath, Synthesis and characterization of wollastonite ($CaSiO_3$)/titanium oxide (TiO_2) and hydroxyapatite (HA) ceramic composites for bio-medical applications fabricated by spark plasma sintering technology, Mater. Today Proc. 45 (2021) 332–337, https://doi.org/10.1016/j.matpr.2020.10.1007.

[69] S.A. Saadaldin, A.S. Rizkalla, Synthesis and characterization of wollastonite glass-ceramics for dental implant applications, Dent. Mater. 30 (2014) 364–371, https://doi.org/10.1016/j.dental.2013.12.007.

[70] S.A. Saadaldin, S.J. Dixon, A.S. Rizkalla, Bioactivity and biocompatibility of a novel wollastonite glass-ceramic biomaterial, J. Biomater. Tissue Eng. 4 (8) (2014) 939–946, https://doi.org/10.1166/jbt.2014.1261.

[71] A. Nommeots-Nomm, P.D. Lee, J.R. Jones, Direct ink writing of highly bioactive glasses, J. Eur. Ceram. Soc. 38 (2018) 837–844, https://doi.org/10.1016/j.jeurceramsoc.2017.08.006.

[72] H. Elsayed, P. Colombo, E. Bernardo, Direct ink writing of wollastonite-diopside glass-ceramic scaffolds from a silicone resin and engineered fillers, J. Eur. Ceram. Soc. 37 (2017) 4187–4195, https://doi.org/10.1016/j.jeurceramsoc.2017.05.021.

[73] W.T. Barbosa, K.V. de Almeida, G.G. de Lima, M.A. Rodriguez, M.V.L. Fook, R. García-Carrodeguas, V.A. da S. Junior, F.A. de S. Segundo, M.J.C. de Sá, Synthesis and in vivo evaluation of a scaffold containing wollastonite/β-TCP for

bone repair in a rabbit tibial defect model, J. Biomed. Mater. Res. Part B Appl. Biomater. 108 (2020) 1107–1116, https://doi.org/10.1002/jbm.b.34462.
[74] H. Akbari Aghdam, E. Sanatizadeh, M. Motififard, F. Aghadavoudi, S. Saber-Samandari, S. Esmaeili, E. Sheikhbahaei, M. Safari, A. Khandan, Effect of calcium silicate nanoparticle on surface feature of calcium phosphates hybrid bio-nanocomposite using for bone substitute application, Powder Technol. 361 (2020) 917–929, https://doi.org/10.1016/j.powtec.2019.10.111.
[75] J. Shen, X. Yang, R. Wu, M. Shen, F. Lu, F. Zhang, Z. Chen, X. Chen, S. Xu, C. Gao, Z. Gou, Direct ink writing core-shell Wollastonite@Diopside scaffolds with tailorable shell micropores favorable for optimizing physicochemical and biodegradation properties, J. Eur. Ceram. Soc. 40 (2020) 503–512, https://doi.org/10.1016/j.jeurceramsoc.2019.09.049.
[76] R. Wu, Y. Li, M. Shen, X. Yang, L. Zhang, X. Ke, G. Yang, C. Gao, Z. Gou, S. Xu, Bone tissue regeneration: the role of finely tuned pore architecture of bioactive scaffolds before clinical translation, Bioact. Mater. 6 (2021) 1242–1254, https://doi.org/10.1016/j.bioactmat.2020.11.003.
[77] A.D. Matchanov, R.S. Esanov, T. Renkawitz, A.B. Soliev, E. Kunisch, I. Gonzalo de Juan, F. Westhauser, D.U. Tulyaganov, Synthesis, structure–property evaluation and biological assessment of supramolecular assemblies of bioactive glass with glycyrrhizic acid and its monoammonium salt, Materials 15 (2022), https://doi.org/10.3390/ma15124197.
[78] F. Baino, D.U. Tulyaganov, Z. Kahharov, A. Rahdar, E. Verné, Foam-replicated diopside/fluorapatite/wollastonite-based glass–ceramic scaffolds, Ceramics 5 (2022) 120–130, https://doi.org/10.3390/ceramics5010011.
[79] M.I. Ramli, A.B. Sulong, N. Muhamad, A. Muchtar, M.Y. Zakaria, Effect of sintering on the microstructure and mechanical properties of alloy titanium-wollastonite composite fabricated by powder injection moulding process, Ceram. Int. 45 (2019) 11648–11653, https://doi.org/10.1016/j.ceramint.2019.03.038.
[80] F. Baino, C. Vitale-Brovarone, Wollastonite-containing bioceramic coatings on alumina substrates: design considerations and mechanical modelling, Ceram. Int. 41 (2015) 11464–11470, https://doi.org/10.1016/j.ceramint.2015.05.111.
[81] ISO 13779-4, Implants for Surgery – Hydroxyapatite – Part 4: Determination of Coating Adhesion Strength, 2002.
[82] E. Garcia, P. Miranzo, M.A. Sainz, Thermally sprayed wollastonite and wollastonite-diopside compositions as new modulated bioactive coatings for metal implants, Ceram. Int. 44 (2018) 12896–12904, https://doi.org/10.1016/j.ceramint.2018.04.100.
[83] Kazuki Orita, K. Goto, Y. Kuroda, T. Kawai, Y. Okuzu, Y. Takaoka, S. Matsuda, Long-term outcome of primary total hip arthroplasty with cementless bioactive glass ceramic bottom-coated implants and highly cross-linked polyethylene: a minimum 10-year analysis, J. Orthop. Sci. 28 (2023) 385–390, https://doi.org/10.1016/j.jos.2021.12.019.
[84] F. Baino, E. Verné, Production and characterization of glass-ceramic materials for potential use in dental applications: thermal and mechanical properties , microstructure , and in vitro bioactivity, Appl. Sci. 7 (2017) 1330, https://doi.org/10.3390/app7121330.
[85] W. Holand, G.H. Beall, Glass-Ceramic Technology, third ed., John Wiley and Sons, Inc., Hoboken, 2020.
[86] Z.W. Loh, M.H. Mohd Zaid, K.A. Matori, M.M.A. Kechik, Y.W. Fen, M.Z. H. Mayzan, S. Liza, W.M. Cheong, Phase transformation and mechanical properties of new bioactive glass-ceramics derived from $CaO–P_2O_5–Na_2O–B_2O_3–SiO_2$ glass system, J. Mech. Behav. Biomed. Mater. 143 (2023), 105889, https://doi.org/10.1016/j.jmbbm.2023.105889.
[87] A. Zocca, B.R. Müller, R. Laquai, A. Kupsch, F. Wieder, S. Benemann, J. Wilbig, J. Günster, G. Bruno, Microstructural characterization of AP40 apatite-wollastonite glass-ceramic, Ceram. Int. 49 (2023) 12672–12679, https://doi.org/10.1016/j.ceramint.2022.12.130.
[88] A. Shearer, M. Montazerian, J.C. Mauro, Modern definition of bioactive glasses and glass-ceramics, J. Non-Cryst. Solids 608 (2023), 122228, https://doi.org/10.1016/j.jnoncrysol.2023.122228.
[89] G. García-Álvarez, J.C. Escobedo-Bocardo, D.A. Cortés-Hernández, J.M. Almanza-Robles, B.A. Sánchez-Escobedo, Effect of wollastonite and a bioactive glass-ceramic on the in vitro bioactivity and compressive strength of a calcium aluminate cement, Ceram. Int. 44 (2018) 19077–19083, https://doi.org/10.1016/j.ceramint.2018.07.186.
[90] S.S. Eldera, N. Alsenany, S. Aldawsari, G.T. El-Bassyouni, E.M.A. Hamzawy, Characterization, biocompatibility and in vivo of nominal MnO_2-containing wollastonite glass-ceramic, Nanotechnol. Rev. 11 (2022) 2800–2813, https://doi.org/10.1515/ntrev-2022-0477.
[91] G. El Damrawi, R.M. Ramadan, M. El Baiomy, Effect of SrO on the structure of apatite and wollastonite phases of $Na_2O–CaO–SiO_2–P_2O_5$ glass system, New J. Glass Ceram. 11 (2021) 45–56, https://doi.org/10.4236/njgc.2021.112003.
[92] A.B. Workie, S.J. Shih, A study of bioactive glass-ceramic's mechanical properties, apatite formation, and medical applications, RSC Adv. 12 (2022) 23143–23152, https://doi.org/10.1039/d2ra03235j.
[93] K. Goto, Y. Kuroda, T. Kawai, K. Kawanabe, S. Matsuda, The use of a bioactive bone cement containing apatite-wollastonite glass-ceramic filler and bisphenol-a-glycidyl methacrylate resin for acetabular fixation in total hip arthroplasty, Bone Jt. J. 101 (2019) 787–792.
[94] A. Faeghi-nia, V.K. Marghussian, E. Taheri-nassaj, M.J. Pascual, A. Dura, Pressureless sintering of apatite/wollastonite-phlogopite glass-ceramics, J. Am. Ceram. Soc. 92 (2009) 1514–1518, https://doi.org/10.1111/j.1551-2916.2009.03018.x.
[95] H. Liu, Z. Fu, K. Yang, X. Xu, M. Bauchy, Machine learning for glass science and engineering: a review, J. Non-Cryst. Solids 557 (2021), 119419, https://doi.org/10.1016/j.jnoncrysol.2019.04.039.
[96] R. Ravinder, K.H. Sridhara, S. Bishnoi, H.S. Grover, M. Bauchy, Jayadeva, H. Kodamana, N.M.A. Krishnan, Deep learning aided rational design of oxide glasses, Mater. Horiz. 7 (2020) 1819–1827.
[97] S. Bishnoi, S. Singh, R. Ravinder, M. Bauchy, N.N. Gosvami, H. Kodamana, N.M. A. Krishnan, Predicting Young's modulus of oxide glasses with sparse datasets using machine learning, J. Non-Cryst. Solids 524 (2019), 119643, https://doi.org/10.1016/j.jnoncrysol.2019.119643.
[98] F. Baino, Porous glass-ceramic orbital implants: a feasibility study, Mater. Lett. 212 (2018) 12–15, https://doi.org/10.1016/j.matlet.2017.10.064.
[99] F. Baino, G. Falvo D'Urso Labate, G.G. di Confiengo, M.G. Faga, C. Vitale-Brovarone, G. Catapano, Microstructural characterization and robust comparison of ceramic porous orbital implants, J. Eur. Ceram. Soc. 38 (2018) 2988–2993, https://doi.org/10.1016/j.jeurceramsoc.2017.12.047.
[100] F. Baino, G.G. di Confiengo, M.G. Faga, Fabrication and morphological characterization of glass-ceramic orbital implants, Int. J. Appl. Ceram. Technol. 15 (2018) 884–891, https://doi.org/10.1111/ijac.12837.
[101] M. Salerno, A. Pietro Reverberi, F. Baino, Nanoscale topographical characterization of orbital implant materials, Materials 11 (2018) 660, https://doi.org/10.3390/ma11050660.